Printed Paper Actuator: A Low-cost Reversible Actuation and Sensing Method for Shape Changing Interfaces

Guanyun Wang[1*], Tingyu Cheng[1*], Youngwook Do[1], Humphrey Yang[2], Ye Tao[1,3], Jianzhe Gu[1], Byoungkwon An[1], Lining Yao[1]

[1]Human-Computer Interaction Institute, Carnegie Mellon University
{guanyunw, tcheng1, hyoungwd, jianzheg, ytao2, byoungka, liningy} @andrew.cmu.edu

[2]School of Architecture, Carnegie Mellon University
hanliny@andrew.cmu.edu

[3]Zhejiang University
Hangzhou, China
taoye@zju.edu.cn

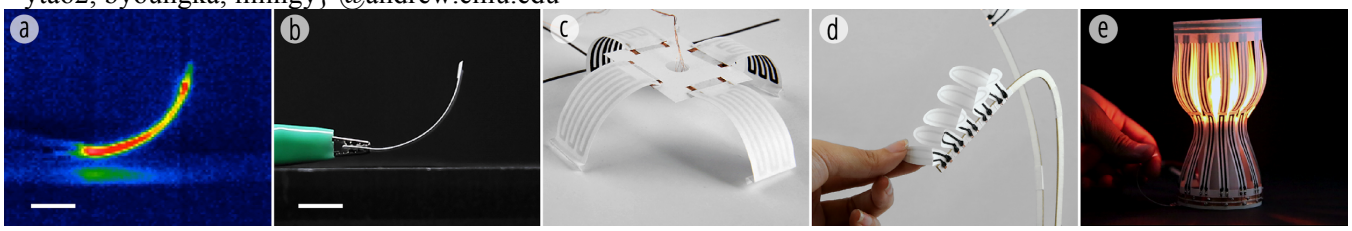

Figure 1. Printed Paper Actuator and its application: (a) Thermal imaging of a bending paper actuator; (b) Color imaging of a bending paper actuator; (c) Modular robot; (d) Artificial mimosa leaves; (e) Transformative lampshade. (Scale bar: 10mm)

ABSTRACT

We present a printed paper actuator as a low cost, reversible and electrical actuation and sensing method. This is a novel but easily accessible enabling technology that expands upon the library of actuation-sensing materials in HCI. By integrating three physical phenomena, including the bilayer bending actuation, the shape memory effect of the thermoplastic and the current-driven joule heating via conductive printing filament, we developed the actuator by simply printing a single layer conductive Polylactide (PLA) on a piece of copy paper via a desktop fused deposition modeling (FDM) 3D printer. This paper describes the fabrication process, the material mechanism, and the transformation primitives, followed by the electronic sensing and control methods. A software tool that assists the design, simulation and printing toolpath generation is introduced. Finally, we explored applications under four contexts: robotics, interactive art, entertainment and home environment.

Author Keywords

Paper actuator; paper interface; 3D printing; 4D printing; shape memory polymer; thermoplastic; self-folding; shape changing.

ACM Classification Keywords

H.5.m. Information interfaces and presentation (e.g., HCI)

INTRODUCTION

Paper is a lightweight, abundant and bio-degradable material. In addition, paper affords rich physical interactions including folding, printing and painting on its surface. In recent years, paper has become increasingly interesting as a material in new interface design, including paper robots [29], paper power generators [11], electronic pop-up books [26], animated origami [25], foldable artifacts [20], and other tangible UIs [35]. While many of these paper systems require customized actuation mechanisms, a missing component for paper-based interfaces is a low-cost, easy to fabricate, flexible to customize, reversible, and electronically-controlled actuator that is embedded within the paper.

This paper presents the design and exploration of a new electrical and reversible paper actuator printed with FDM 3D printers (Figure 1). The actuator is composed of inexpensive materials, such as common paper and off-the-shelf thermoplastic printing filaments. The fabrication process is fast and straightforward, which requires a single layer printing with a desktop FDM printer. Our paper actuator can be easily embedded into everyday objects to enable new types of "paper-based shape changing interfaces", such as pop-up books, toys, packages, origami robots, and lampshades enhanced with motion, transformation, and rich interactivities.

The paper actuator presented in this paper is based on a few well-known structural principles and mechanisms of a material: the bilayer bending actuation structure, the shape memory effect of thermoplastic material, and the current-driven joule heating phenomenon of a conductive printing

* The first two authors contributed equally to this work.

CHI 2018, April 21–26, 2018, Montreal, QC, Canada

ACM 978-1-4503-5620-6/18/04…$15.00
https://doi.org/10.1145/3173574.3174143

filament. Developing, characterizing, evaluating, and showcasing interactive paper actuators based on these aforementioned material principles are some of the major contributions of this paper.

		Fabrication Methods		
		3D Printing	Laser Cutting and Layer Stacking	Inkjet Printing (2D Printing)
Stimuli Type	Global Heating	Pattern formation [41, 42]	Uniform heating origami [2, 32]	Self-folding polymer sheets [14, 15]
	Local Heating	Our method	Self-folding machines [5, 6]	Self-folding 3M tape [20]

Table 1. Summary of recent progress on actuation material and method with heat-actuated thermoplastic.

It is important to highlight the differences between our approach and other actuators developed from heat-actuated thermoplastic within and beyond HCI. Table 1 shows an overview of recent developments on thermal-induced actuation methods with thermoplastics. If we look at both the stimuli type and the fabrication method, our approach is novel in terms of adapting 3D printing methods to create locally controllable actuators. Compared to FDM 3D printing, laser cutting requires tedious multi-layer printing, aligning, and bonding processes that heavily demand time and accuracy; inkjet printing affords less flexibility in the actuator design and the actuation is limited.

CONTRIBUTIONS AND LIMITATIONS

The main contributions of the work include the following:

1. A novel reversible paper actuation technology based on the bilayer bending actuation structure, the shape memory effect of thermoplastic, and the current-driven joule heating phenomenon of a conductive printing filament. To our knowledge, it is the first 3D printed paper actuator that uses FDM printing filaments as both the resistive heating element and actuator.

2. A set of shape changing and actuation structures, to combine our actuation technique with the flexibility of paper handling, including cutting, folding, scoring, bending, etc. The structures cover folding types (e.g., curve folding, sharp folding), construction methods (e.g., pattern method, kirigami method), and properties (e.g., elasticity, permeability).

3. Several application scenarios that demonstrate the use of our paper actuator techniques for actuating interactive objects, such as paper toys, animated pop-ups, paper robots, and responsive home appliances.

However, the resulting techniques are also subject to limitations. The filament does not stick to the paper covalently and it can be peeled off especially if the 3D printer's nozzle height is not adjusted perfectly during the printing. Since the resistance of the filament is relatively high (~0.6Ω/cm volume resistivity), the actuator requires relatively high voltage (ranging from 40V to 130V for the size of the actuators we have tested). Thus, the maximum size of the actuator is constrained. Finally, as graphene embedded in PLA filaments expands in a heated printing nozzle, it tends to cause nozzle clogging more frequently than normal PLA filaments.

PAPER ACTUATOR METHOD

Design and Fabrication

Figure 2 shows the structure of the actuator: a bi-layer structure with a paper substrate and a conductive thermoplastic layer.

In terms of the materials we used: for most of the samples shown in this paper, we use normal copy paper as the substrate. However, we can use thin-plastic film (e.g., PET film 0.5mm) instead of obtaining higher rigidity as well. For the printing filament, we chose a graphene PLA composite filament (Conductive Graphene PLA Filament, Black Magic 3D). We used a MakerBot Replicator 2X with a 0.5 mm printing nozzle tip to print the actuator. It is important not to use a standard 0.4 mm nozzle tip as the clogging issue will be severe due to the expansion of graphene in the heated nozzle.

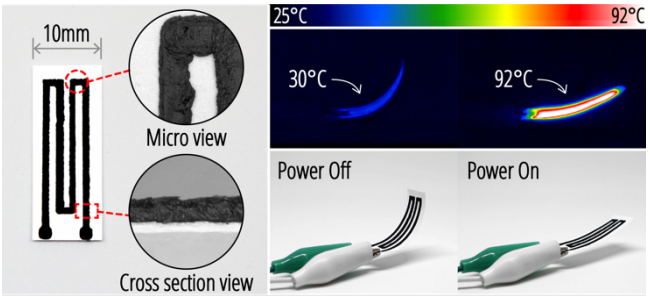

Figure 2: Composition of the paper actuator

Figure 4 describes the fabrication process and the performance of our paper actuator at each step.

Step 1: Printing (Figure 4-a1)

- Place a paper substrate in a 3D printing platform. As the paper has a micro structured surface, and the filament has graphene fibers, the two materials bond relatively well. If the substrate is a smooth plastic film, we must create a surface microstructure by either laser etching or mechanical sanding (Figure 3).

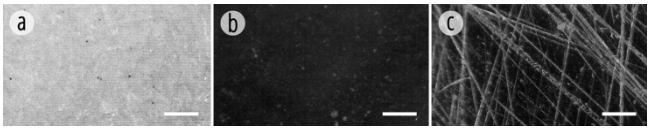

Figure 3. Microtexture on the sample matters: (a) copy paper; (b) plastic film before sanding, which does not work well; (c) plastic film after sanding. (Scale bar: 1mm)

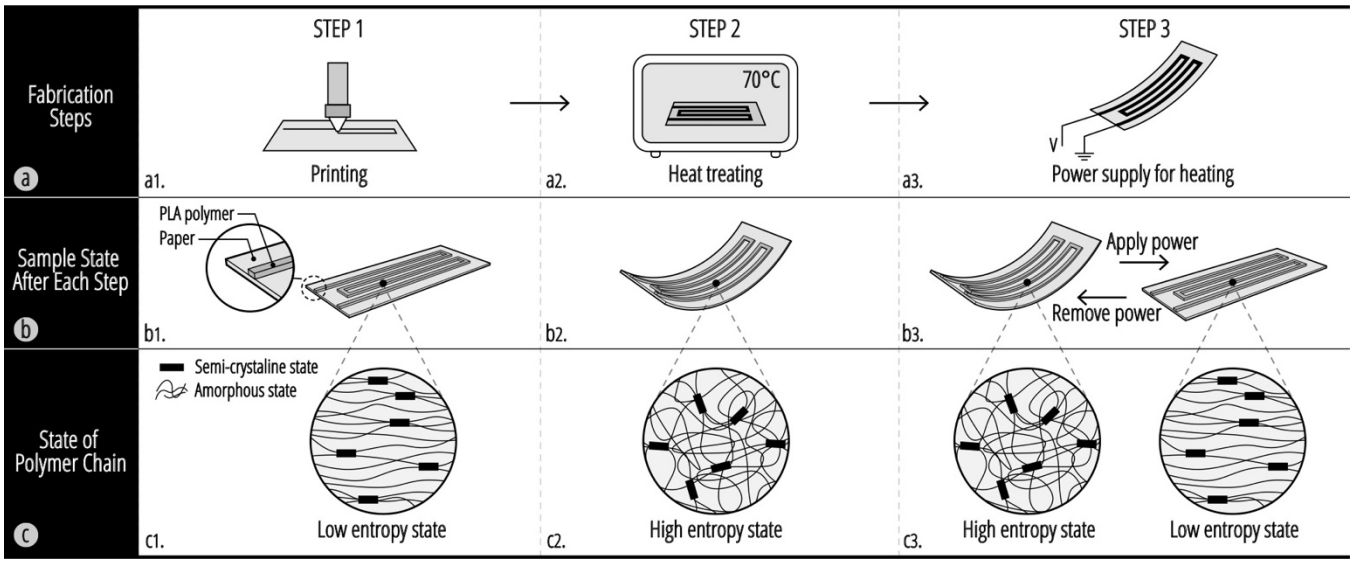

Figure 4. Paper actuator method: (top row) fabrication process; (middle row) material sample state after each step; and (bottom row) material mechanism based on shape memory and resistive heating.

- Generate the printing tool path with our design tool, and print in a single-layer on a FDM printer. The printing speed is 3000 mm/min, with a heating temperature of 245 ~ 250 °C, a printing toolpath thickness of 0.5 mm, and a single layer height of 0.2 mm.

After step 1, the actuator is flat (Figure 4-b1).

Step 2: Initialize the Bending angle (Figure 4-a2)

- Preheat a convection oven to 70 °C.
- Place the samples inside the oven for a heat treatment. After 10 seconds of continuous heating, pick it out of the oven immediately with a tweezer.
- Wait for about 10s until the paper bends upwards and sets its final angle. To preserve the shape memory effect which contributes to the reversible bending, it is critical not to overheat the plastic and cause it to melt.

After step 2, the actuator bends upwards and stays at its maximum bending angle (Figure 4-b2).

Step 3: Providing power for the reversible actuation (Figure 4-a3)

- Solder the connection point following instructions shown in Figure 5.
- Connect to the power supply via the control circuits.

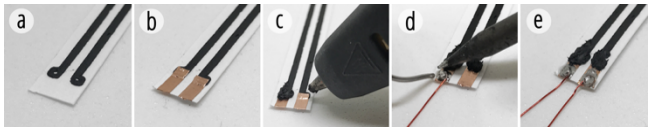

Figure 5. (a) Connection point; (b) Place copper tape; (c) Connect the actuator with copper tape with fused conductive PLA filament; (d) Solder stripped magnetic wire tip to the copper tape; (e) The finished look.

During step 3, when proper power is provided, the actuator bends back flat from its initial maximum bending angle; and it returns to its maximum bending angle once the power is withdrawn (Figure 4-b3).

Material Mechanisms - Shape Memory and Resistive Heating

Although the structure of the actuator is rather simple, different physical phenomena undergo each step. Therefore, we describe the material mechanisms that are related to our actuation functions based on aforementioned three steps for fabrication (Figure 4c).

Step 1: Printing (Figure 4-c1)

As the printer deposits the filament on the paper, the filament is melted and then quickly cools down to the temperature of the paper substrate. Due to its rapid cooling, the printed lines have built in inherent thermal stress.

Step 2: Initializing the bending angle (Figure 4-c2)

This involves heat treating to release the residual stress within the thermoplastic. Due to the release of the residual stress, the plastic layer tends to shrink along its longitudinal direction; However, since the paper layer is unaffected by heat, it acts as the strain-limiting layer, thus the dimensional changes of the plastic layer are translated into a bending motion. In the end, as the material cools down, the sample will stay bent. This is its programmed initial shape.

Step 3: Providing power for reversible actuation (Figure 4-c3)

Initially, the actuator is in its bended state. When electrical power is provided to the conductive printed layer, this layer functions as a resistive heating element which causes itself to soften. It heats up and softens more efficiency compared to resistive heater and plastic composite [9, 20] as the current dissipates through the inside of the plastic through the graphene composite. As the printed layer becomes softer, it loses its stress and cannot hold the bended shape anymore because the constraining paper layer tends to return to its flat state.

Once the power is withdrawn, the thermoplastic layer will cool down and pull the flat paper to its bended state again. This happens because of the shape memory effect of the thermoplastic [20, 32]. Hence, the aforementioned flattening and bending are repeatable processes.

Primitive Structure

We designed multiple groups of actuators with this technique. These actuator primitives serve as transformation references for the applications described in the later section.

Folding Types

The first category we developed is based on the folding types - sharp folding or curve folding (Figure 6).

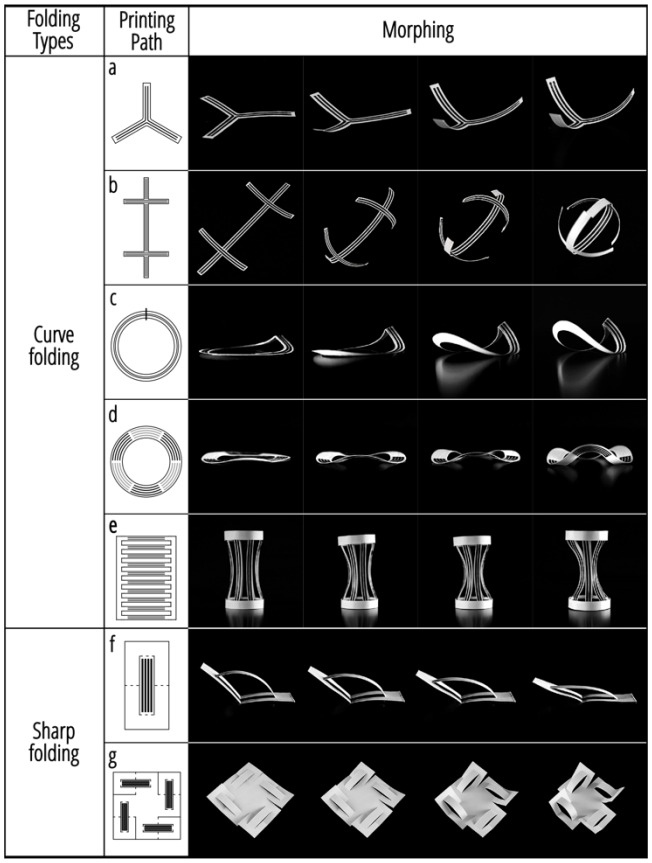

Figure 6. Folding Types

- Curve Folding

These are transformations based on line combinations, and can form smooth curved structures. The lines can be combined to form different curved 2.5D or 3D geometries. For example, Figure 6b shows the primitive pattern that reversibly transforms a flat shape frame into a curved frame and results in forming a ball shape; Figure 6e shows the primitive design that transforms a cylinder wire frame into a concave cylindrical curved frame. Later we show a lampshade design based on the pattern shown in Figure 6e.

- Sharp Folding

By combining folding with curved actuator, we developed sharp folds (Figure 6f). Figure 6g shows that through cut-and-fold, we can achieve four sharp folding actuators with one piece of paper.

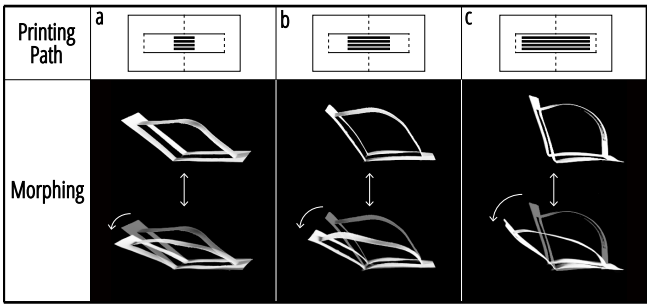

Figure 7. Tunable maximum folding angles

Furthermore, we can tune the maximum folding angle by varying the length of the bending actuator (Figure 7). With our measurements, the sharp angle primitives can achieve 95-160° and the tested effective actuator length is 4-6cm.

Construction Methods

In this section, we categorize the primitives based on how the actuators are constructed. By printing actuator patterns on both the inner and outer sides of the paper, or applying some cuts on the paper, we constructed paper actuators that can dynamically morph between different shapes or serve as pop-up actuators.

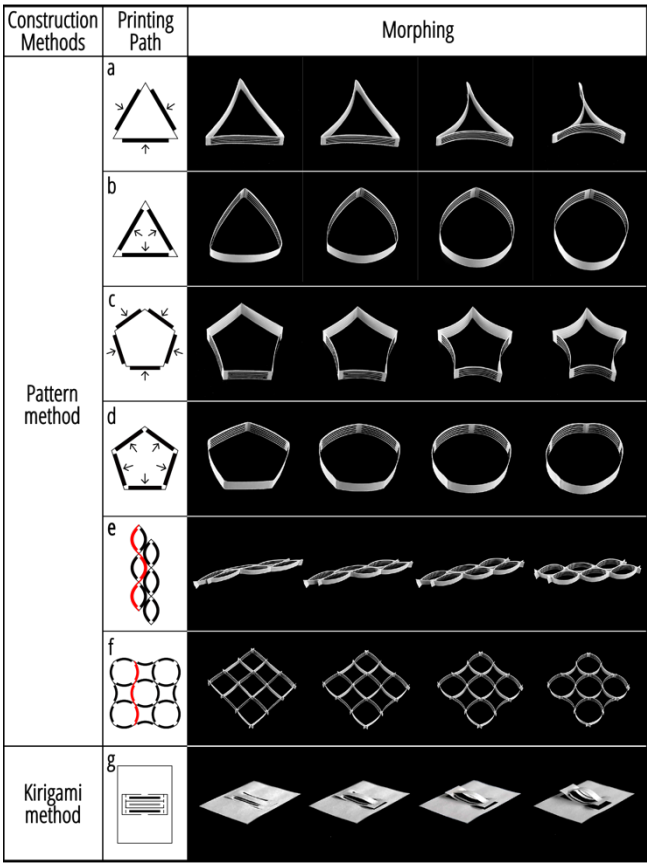

Figure 8. Construction Methods

- Pattern Method

This group explores how same pattern on different printing areas within the same geometry can cause different transformation. For example, a pentagon transforms into a star (Figure 8c) when filament is printed outside the paper, a pentagon shape (Figure 8d) transforms into a circle shape when the filament is printed inside. Morphing between different patterns enables applications to acquire dynamic and symbolic display.

In addition, Figure 8e and 8f show a more complex pattern combination. These patterns require manual cut and snap-fitting based assembly. We demonstrate that a group of honeycomb structures transform into a line (Figure 8e), or a matrix of squares transforms into a matrix of circular units (Figure 8f). The basic fabrication process includes a set of paper strips with cut slits that can be interlinked with a manual assembly process (e.g., Figure 8e has four such strips). To trigger the transformation, we can either apply an external heat source or connect printed traces with magnetic wires for electrical control.

- Kirigami Method

The kirigami actuator is interesting as it does not waste any paper (Figure 8). By cutting and distributing the actuator at different regions, we can create various actuation patterns. Later in the application section, we show a popup art based on the cascading kirigami actuator.

Properties

Based on how the paper actuators perform, we can also categorize them according to the tunable properties.

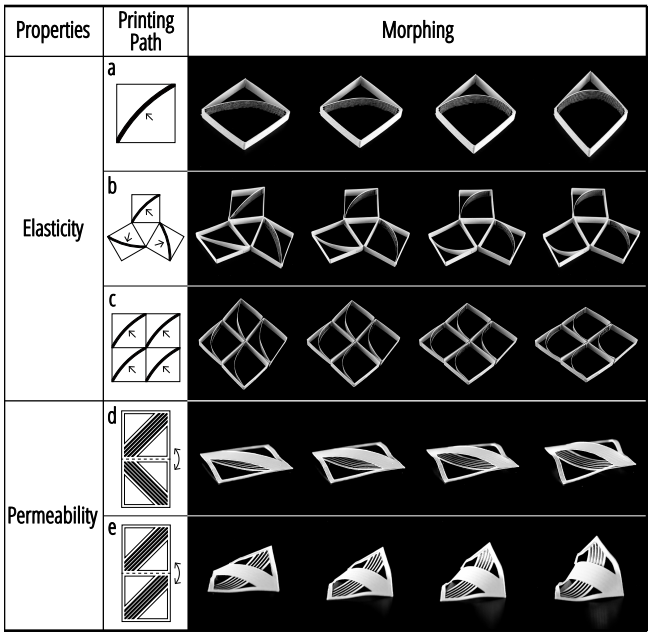

Figure 9. Tunable Properties

- Elasticity

Here, we use elasticity to describe the primitive behaviors that resemble rubbers. Its body resists the deforming force as the thermoplastic heats itself up, and returns it to its original size and shape when the heating current is removed (Figure 9). Unlike the morphing lines, these primitives experience smaller elastic deformation, and some do so in a collective manner. While tunable elasticity has an interesting design potential for tessellation-based actuators (Figure 23b), its bending angle is smaller than others such as curve folding. This is due to the friction in the folding hinges of the frame, and between the sample and the floor.

- Permeability

These patterns tune the porosity, or permeability by having two stacked layers bending towards the opposite directions.

MATERIAL PERFORMANCE

Effects of Geometry on the Maximum Bending angle

From Figure 10, we concluded that the W/L ratio is critical for deciding the maximum bending angle of the actuator. Within our tested range, as the W/L increases (relatively thicker traces), the bending angle decreases. Below, we will detail the experimental setup.

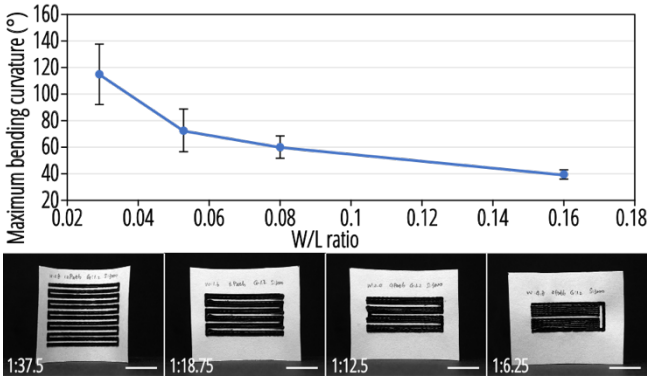

Figure 10. Maximum bending angle changes according to the W/L ratio of the actuator. (Scale bar: 10mm)

To investigate the relationship between the maximum bending angle and the width over length (W/L) ratio of each strip, we printed samples with four different W/L ratios: 1:37.5, 1:18.75, 1:12.5, and 1:6.25.

For the reason behind the chosen ratios, the chosen line length and the limitation on the width range of the lines are the important factors. First, we decided a length of 30mm which is the average effective length in our primitives; we then decided the width range of the lines: printing resolution allows a certain minimum width (0.4mm), and the bending performance decides the maximum width (based on our tests, lines wider than the chosen maximum width will lose bending orientation controllability). Based on these dimensional factors or limitations, four chosen samples are 30mm in length, with line width of 0.8mm, 1.6mm, 2.4mm and 4.8mm respectively.

Moreover, all the samples contain the same printed area, 288 mm^2 and they are single-layer printed with a printing speed of 3000 mm/min on a piece of paper of size 45 mm by 35mm.

Response Time

A resistive heating based actuator's response speed is relatively slow compared to more common electromagnetic actuators. Recently, *Foldio* [20] shows that a shape memory polymer based actuator takes 3 minutes to fully recover from its maximum bending angle to its flattened state, while *uniMorph* [9] did not report its response time. More literature in shape memory actuators also report a slow response in general [27]. For a recovery from its maximum bending state, PU/polypyrrole system takes 50 seconds [37], and SMP stent takes 100 seconds [36].

We show that our actuator's average full recovery time is 20 seconds (Figure 12&13). However, for most of our applications, we do not need the full recovery time and we control the cycling time at around 17 seconds.

ELECTRONIC CONTROL

Power Consumption and Control

We try to determine the ideal normalized power per unit area (P_n), which can be applied to calculate the required driving voltage for any given actuator geometry, to enable a consistent performance and minimized decay of the paper actuator. Heating the actuator insufficiently cannot make the sample flatten completely, while overheating diminishes the shape memory effect of the thermoplastic and destroys the actuator.

Experiment Design

We chose a sample with a line thickness of 1.2 mm, line numbers of four, line length of 30 mm, printing speed of 3000 mm/min, printing layer of one, and total resistance of 4195 Ω at room temperature. We ran six experiments on the sample. The driving voltage options of the experiments were from 50V to 100V with a 10V incremental step. We ran three cycles of unfolding and folding, and recorded both the full color video and the thermal imaging video at the same time. At the end of the experiments, we plotted the bending angle changes and the temperature changes as a function of time with various voltage options during three cycles (Figure 12&13, respectively).

Experiment Analysis

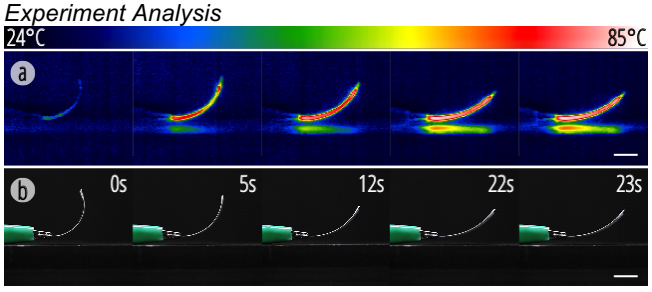

Figure 11. Color and thermal imaging of the bending angle changes according to the voltage of 80V. (Scale bar: 10mm)

Figure 11 shows the angle changes of one cycle when the filament is heated with an 80V driving voltage. Figure 11 indicates that the thermoplastic layer is used as a resistive element to generate the heat necessary for a change in the stiffness of the material itself - and in turn for actuation — of the paper actuator. The total heat on the resistive material will accumulate with time, which causes the continuous decrease of the bending angle. However, because of the open exposure and energy exchange with the environment, each sample will reach equilibrium with the environment and its angle will eventually stay constant. The ideal driving voltage is that which enables the sample to reach equilibrium when it is perfectly flat.

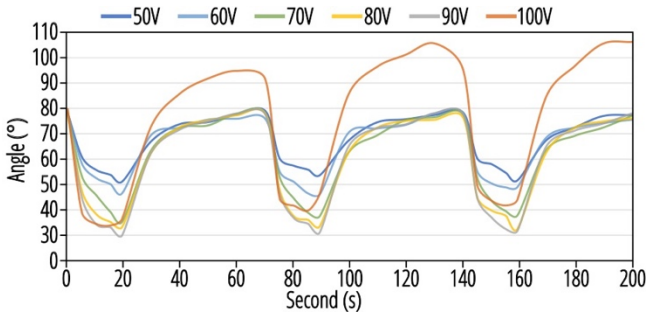

Figure 12. Bending angle changes as a function of time with various voltage options during the three cycles.

Figure 12 shows that the bending angle is related to the driving voltage of the paper actuator. We set the standard of a proper voltage as one that enables the maximum range of changes and stable performance over multiple cycles. Since a voltage between 80V to 90V exhibits maximum angle change (~50°) and consistent performance without decay, we conclude that a voltage between 80V to 90V is appropriate. Bending angle was measured using ImageJ software with side-view photos of an actuator. Based on the measurement of the sample's resistance and surface area (A = 144 mm^2), we can calculate ***the minimum normalized power per area (P_n) is 1.06×10^{-2} W/mm2.*** P_n is our standard value to determine the proper power for a given actuator geometry.

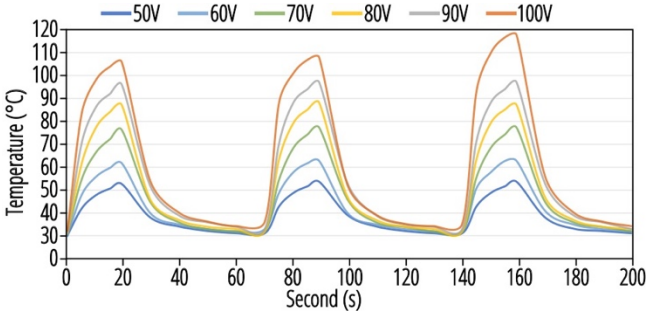

Figure 13. Temperature changes according to time with various voltage options during three cycles.

Figure 13 plots the same set of experiments to determine the relationship between actuator temperature and heating time. For the proper voltage range of 80V–90V (the concluded ideal voltage range for our testing sample), ***the ideal actuator heating temperature is between 85°C to 95°C***. This temperature becomes a useful reference when we determine the power value for a given actuator.

Touch Sensing

The conductivity of the printing filament enables our paper actuators to have capacitive property. The capacitance of the conductive material changes if there is contact with another conductive object. This allows us to detect the presence of a finger touch on a paper actuator sample. We modified the experimentation in [17, 30] to implement a capacitive sensing technique. We use a transient response of the first order RC circuit to implement a capacitive sensor using an Arduino Uno Rev3 as a microcontroller (Figure 14). After calibration steps regrading capacitance values, we observed 196 times correct sensing results out of 200 times trials.

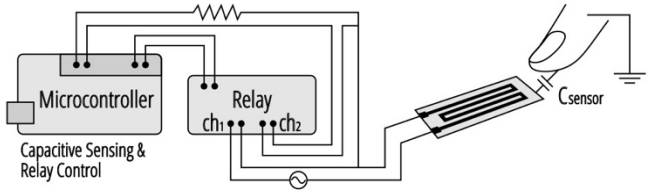

Figure 14. Capacitive sensing and actuation system

Additionally, a sample can be actuated with touch interaction (Figure 15). We use a relay control to combine this sensing circuit configuration and the actuation circuit configuration. Once a touch event occurred, channel 1 opens the capacitive sensing circuit and channel 2 closes the actuation circuit.

Figure 15. Capacitive sensor demonstration

Finger Sliding Sensing

A human body is not only capacitive but also resistive. The total resistance of a paper actuator changes if a finger contacts its printed conductive material. The resistance variation caused by touching a different part of the actuator results in sending a corresponding input voltage to an analog signal reader on a microcontroller. We take advantage of this property and modified the experimentation in [30] to implement a physical slider device (Figure 17). By mapping the range of voltage changes in the cursor position range, the cursor can be controlled simply by finger sliding on the paper actuator sample.

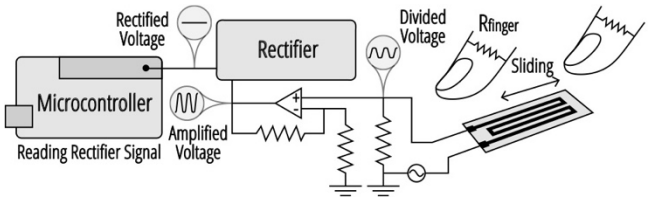

Figure 16. Finger sliding sensing system

We design a circuit to measure a sample's resistance in real time (Figure 16). Given AC 30V power supply, a resistor (47Ω) of which resistance is 250 times as low as a paper actuator (~ 12kΩ) is connected in series with the actuator to divide voltage. The resistor has a relatively constant resistance regardless of being heated or not. However, due to the relatively high resistance of a finger (>1MΩ) compared to the sample's resistance, the total resistance change is not significantly large when a finger touches a different part of the sample. This leads to only a subtle current change on the circuit. To have a distinguishable current change, the divided voltage is amplified. The rectifier bridged with the resistor converts the amplified AC voltage to a DC voltage. The microcontroller reads the input voltage from the rectified voltage. We can draw the resistance of the sample by measuring the electric potential and recognize the location of a finger touch event. The best performance achieved to exhibit sliding sensing is to recognize different positions of a finger touch event by 40mm-long interval with an 80mm-long sample.

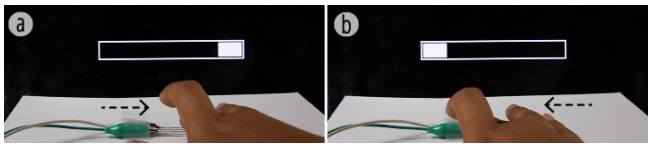

Figure 17. Finger sliding sensing demonstration

In all the sensing modes mentioned above, we do not heat up the sample so users can safely touch them. However, when heated during the actuation, the sample can reach up to 70-95°C. It is not recommended to touch the actuator during this stage.

Bending Angle Detection

We found that as the result of a sample being heated and actuated, the resistance of the sample increases. Figure 18 shows the changes of resistance according to the changes in the actuator's bending angle. As a result, self-angle sensing is achieved based on the relationship between the sample's resistance change and bending angle (Figure 19). The changes of resistance are detected with the same circuit diagram discussed in Figure 16. By modifying the experimentation in [23], we utilized this characteristic to implement our bending angle detection technique.

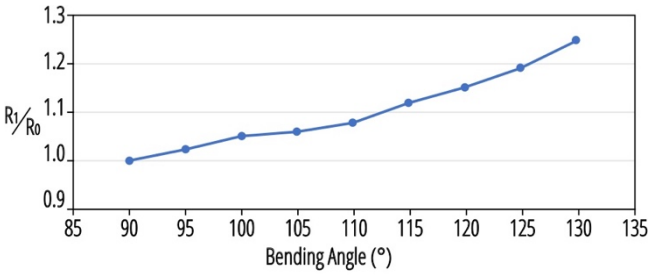

Figure 18. Resistance changes according to bending angle of the sample (R_0: Resistance on an initial state; R_1: Resistance according to bending angle).

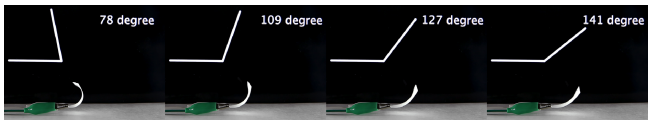

Figure 19. diagram for bending angle detection

To obtain the accuracy of bending angle detection, we used ImageJ to measure bending angle and compared target angle and measured angle. We collected the data from 3 trials and averaged the measured data for each target angle. The result shows ±5° error rate with 1.5° standard deviation at the largest (Figure 20).

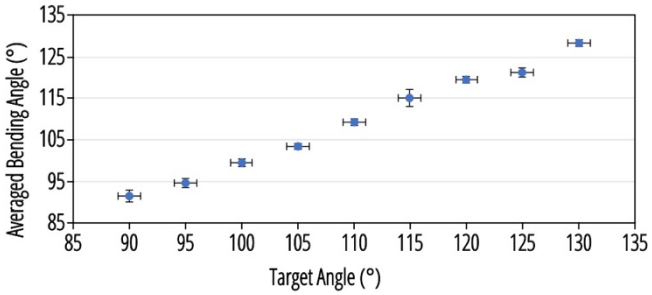

Figure 20. Comparison between target bending angle and observed bending angle.

DESIGN SOFTWARE

Geometrical Interpretation of the Paper Actuator

In our software, two types of actuators are described: a bending actuator (Figure 21a) and a folding actuator (Figure 21b). Curvature along the printed line is constant, namely the profile of the actuator resembles an arc. By finding the radius of the circle encompassing the arc, the bending transformation can be conveniently described and represented. In folding actuators, as actuation angle in folding actuators is separated from the bending angle, an extra step to convert actuation angle into bending angle is required.

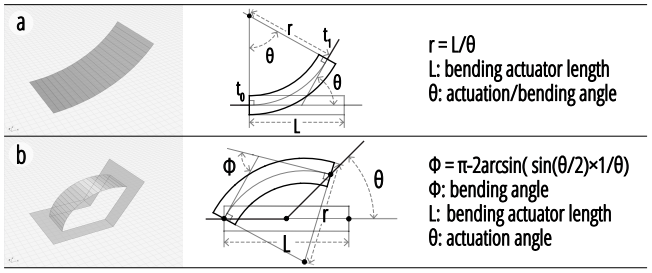

Figure 21. Geometry behind transformation: (a) folding actuators; (b) sharp angle actuators.

Walkthrough

Using Rhinoceros 5 as environment and Grasshopper as intermediate interface, the software contains several modules to scaffold the design process of printed paper robots. The software, as demonstrated in Figure 22, streamlines such a design process by generating actuators in 3D space, simulating their transformation, and producing files for fabrication.

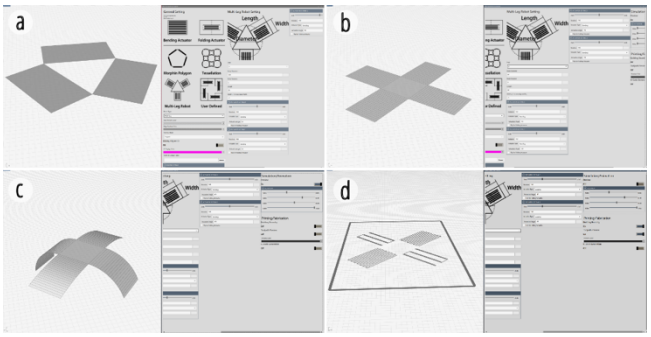

Figure 22. Design walkthrough: (a) Design the form factor; (b) specify the actuation behavior; (c) simulate the actuation; (d) generate printing toolpaths.

Design the form factor: Users can choose from the provided templates - single actuator, morphing or tessellation pattern, and multi-leg robot - to begin with, or can define and input their own robot into the software.

Specify the actuation behavior: With designers specifying each actuator's type and desired actuation angle, an interpolation algorithm will provide proper fabrication parameter values and performance data from a database of pre-tested parameter sets.

Simulate the actuation: The constructed robot can be previewed, tested, and modified in real time. To simulate the transformations of actuators, we segment the actuator into smaller pieces and mathematically describe its' displacement. Designers have control over each actuator with a value between 0 (relaxed) to 1(fully actuated), hence enabling the animation of the robot's transformation and movement.

Generate printing toolpaths: Lastly, the software can automatically generate and optimize the toolpath for fabrication, and produce G-Code for printing.

Currently, the software's application is limited to linear actuator connections.

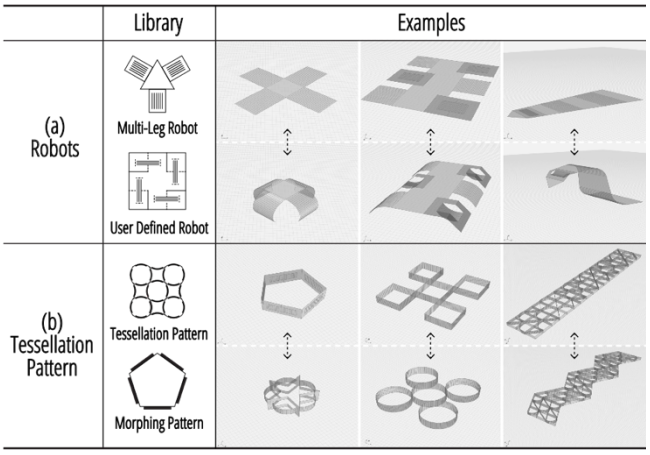

Figure 23. Design possibilities: (a) Robots design; (b) tessellated morphing pattern.

Design Features - Robots and Tessellation

We use two design contexts as examples to show the possibilities for design: robots and tessellated morphing pattern. With the software, a variety of form factors with two actuator types can be tested out quickly (Figure 23).

APPLICATIONS

We developed a few applications to demonstrate the potential usage of our printed paper actuator. Applications are chosen to exemplify different sensing and actuation methods of the paper actuator.

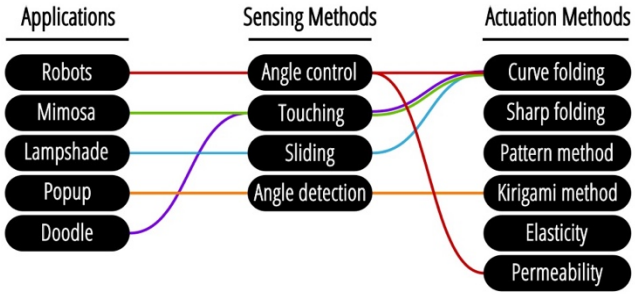

Figure 24. Application overview

Robots - Modular and Reversible Actuation

With the primitive of a single morphing line or morphing pattern discussed previously, we achieved a variety of modular robots (Figure 25). These robots combine paper actuators with paper handling techniques, such as cutting (permeability), curve folding, etc. The reversibility, response time, and power control methods are based on our previous tests. One cycle of the movement takes on average 15 seconds. Compared with other thermoplastic based robotic actuators, it can achieve a faster movement. For just half the motion cycle (recovery time), *Foldio* takes 3 minutes [20], the PU/ polypyrrole system takes 50 seconds [37] and the SMP stent takes 100 seconds [36].

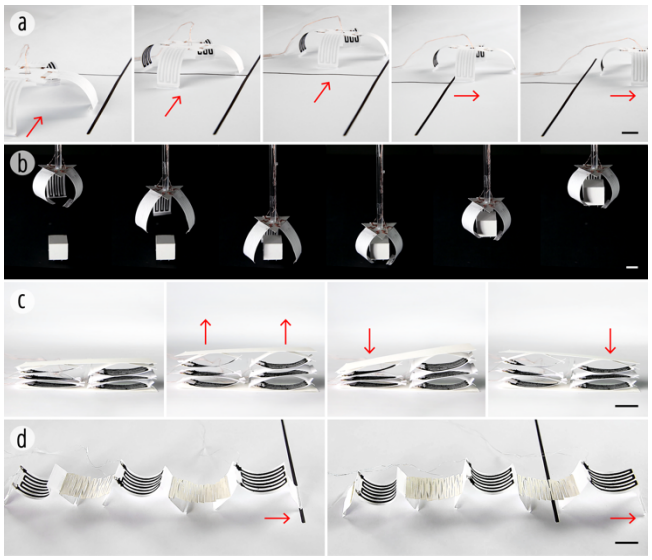

Figure 25. Modular robots (Scale bar: 20mm)

Mimosa - Touch Sensing and Sequential Actuation

We developed an artificial plant, a mimosa tree branch (Figure 26). When one of the mimosa's leaves is touched, a sequential actuation is triggered to see each pair of leaves unfold one after another.

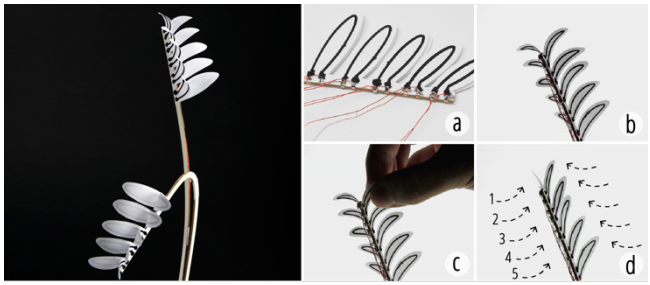

Figure 26. Responsive artificial plants - mimosa.

Lampshade - Sensing Slider, Volumetric Transformation and Tunable Light

A lampshade is developed to showcase how a transformable volumetric shape can be integrated with slider sensing (Figure 27). The light can be switched on by an active switch printed with our paper actuator material. When users slide across the slider, the lampshade changes in form to either expose more or less light.

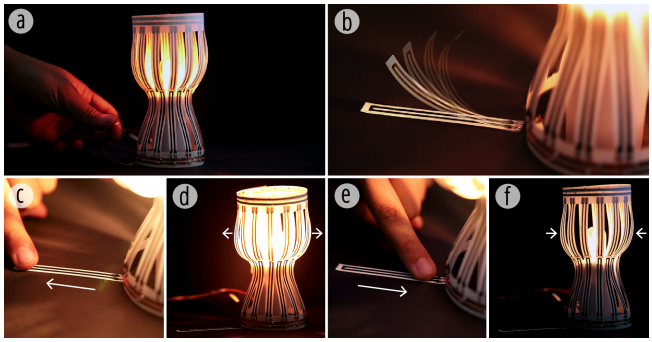

Figure 27. Lampshade

Pop-up Art - Cascading Actuator by Kirigami

One advantage of our technique is that we can quickly and precisely print complex 2D patterns. We implemented a kirigami actuator based pop-up art. Electricity can trigger a paper sculpture to grow out of a flat sheet (Figure 28).

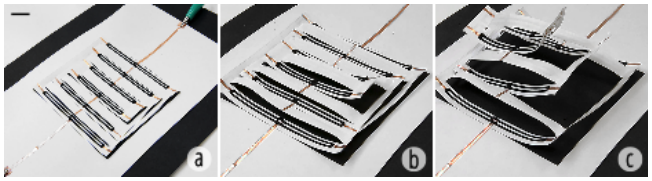

Figure 28. Popup Art (Scale bar: 20mm)

Doodle Actuator - Beyond Printing

Compared to a 3D printer, a pen sometimes is an easier option to use with paper, especially for situations when more expressiveness and less accuracy are required. By loading a conductive filament to a fused deposition pen (Soyan Professional 3D pen), we can draw circuits on paper

(Figure 29). These circuits can function as aesthetic features, sensors, actuators, or just conductive traces. Figure 29 shows a hedgehog drawing taking less than one minute. When the spikes are touched, the red nose lights up and the spikes stand up. A touch sensor, responsive lighting, and actuation are easily integrated in one piece of paper art.

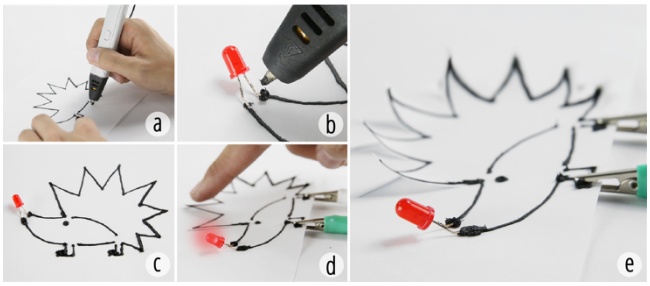

Figure 29. Doodle Actuator

RELATED WORK

Our work builds on previous work in shape changing materials, especially on printed actuation techniques, and thermoplastic based actuators.

Material-based Shape Changing Interfaces

Recently, a variety of non-electromagnetic motor based actuators have been introduced in HCI. For instance, *PneUI* [38], *aeroMorph* [22] and *Printflatables* [28] introduce pneumatic driven actuators based on soft composite materials; *Surflex* [3] and *Electronic Popables* [26] demonstrate shape memory alloy (SMA) based actuators to explore programmable surfaces; beyond traditional materials, biomaterials [34], chemical materials [10] and living materials [39] are increasing their presence in HCI. With our printed paper actuator, we hope to add one more technique for enabling the fast and low cost prototyping of shape changing interfaces.

Printed Actuators

Among material-based actuators in recent HCI literature, plenty of them involve 3D printing (e.g., *Cilllia* [21], *bioLogic* [33, 39], *aeroMorph* [22]), and many others involve 2D printing (e.g., *uniMorph* [9], *Foldio* [20]). Our printed actuator technique adds an additional contribution to this group of works, by utilizing conductive thermoplastic printing filament on a desktop FDM printer as both the actuation and resistive heating elements.

Paper Actuating

Paper is favored by researchers for its wide accessibility, affordance as a creative crafting material, and biocompatibility. Within HCI, paper has been explored as actuating artifacts [19, 26], material options for I/O devices [20, 29], rapid prototyping materials [12, 31] and interaction design toolkits [35].

Different techniques to actuate paper have been introduced, including humidity sensitive coating [1, 8], shape memory alloy [13, 24, 25], pneumatic actuators [18], ferrofluid-impregnated paper actuator [4], shape memory polymer paper actuator [20], magnetization [19], etc. Building on top of these existing enabling technologies, we introduce a shape memory thermoplastic paper composite, with its own capability of conducting and generating heat, actuation, touch sensing and shape sensing.

Thermoplastic Based Interfaces

Thermoplastic is a widely-used material type in fast prototyping, daily life, engineering, and construction. Beyond injection modeling and fused deposition modeling based 3D printing, thermoplastic has been introduced in novel uses in HCI. *HotFlex* [7] utilizes its viscoelastic property above glass transition temperature to reshape 3D printed parts; *ShrinkyCircuits* [16] utilizes its non-reversible shrinking to fast prototype miniaturized circuits; and a shape memory polymer based popup by microwave heating [40].

Foldio [20] introduces a shape memory actuator by combining 3M tape with inkjet-printed heating circuits. We share the common design vision with *Foldio* actuators as both are low-cost, easy-to-print and heat-driven actuators. While *Foldio* takes 3 mins to fully recover, our actuator takes averagely 20 secs. Further, *Foldio* is a trilayer with 3M tape as the actuator and conductive ink layer as the heater; ours is a bilayer and the printed pattern functions as both an actuator and a heater. Our approach can speed up the heat dissipation (unlike our heater exposed to the open air, the heater in *Foldio* is buried between the substrate and the 3M tape) and thus reduce the recovery time; it also gives us more controllability over the transformation as the printing orientation affects the bending behavior.

Beyond HCI, shape memory thermoplastic has been used as a non-reversible actuator [2, 32]. Researchers also embedded resistive heating components to selectively heat regions and achieve sequential self-folding [5].

CONCLUSION

In this paper, we present a paper actuator, which is a composite material printed by desktop FDM 3D printers. While many approaches to actuating papers have been introduced before, the main contribution of our paper is the design of the composite, which seems simple but indeed combines three physical phenomena: electrical resistive heating of conductive thermoplastic, shape memory effect, and bi-layer actuation. We hope to introduce our paper actuator as a low cost and easy-to-fabricate enabling material to the community.

REFERENCES

1. Amjadi, M., Sitti, M. 2016. High-Performance Multiresponsive Paper Actuators. *ACS nano 10*, 10202-10210.
2. An, B., Miyashita, S., Tolley, M.T., Aukes, D.M., Meeker, L., Demaine, E.D., Demaine, M.L., Wood, R.J., Rus, D. 2014. An end-to-end approach to making self-folded 3D surface shapes by uniform heating. In *Proceedings of the 2014 IEEE International*

Conference on Robotics and Automation (ICRA), 1466-1473.

3. Coelho, M., Ishii, H., Maes, P. 2008. Surflex: a programmable surface for the design of tangible interfaces. In *Proceedings of the CHI'08 extended abstracts on Human factors in computing systems*, 3429-3434.
4. Ding, Z., Wei, P., Chitnis, G., Ziaie, B. 2011. Ferrofluid-impregnated paper actuators. *Journal of Microelectromechanical Systems 20*, 59-64.
5. Felton, S., Tolley, M., Demaine, E., Rus, D., Wood, R. 2014. A method for building self-folding machines. *Science 345*, 644-646.
6. Felton, S.M., Tolley, M.T., Onal, C.D., Rus, D., Wood, R.J. 2013. Robot self-assembly by folding: A printed inchworm robot. In *Proceedings of the 2013 IEEE International Conference on Robotics and Automation (ICRA)*, 277-282.
7. Groeger, D., Chong Loo, E., Steimle, J. 2016. Hotflex: Post-print customization of 3d prints using embedded state change. In *Proceedings of the CHI 2016*, 420-432.
8. Hamedi, M.M., Campbell, V.E., Rothemund, P., Güder, F., Christodouleas, D.C., Bloch, J.F., Whitesides, G.M. 2016. Electrically Activated Paper Actuators. *Advanced Functional Materials 26*, 2446-2453.
9. Heibeck, F., Tome, B., Della Silva, C., Ishii, H. 2015. uniMorph: Fabricating thin film composites for shape-changing interfaces. In *Proceedings of the UIST 2015*, 233-242.
10. Kan, V., Vargo, E., Machover, N., Ishii, H., Pan, S., Chen, W., Kakehi, Y. 2017. Organic Primitives: Synthesis and Design of pH-Reactive Materials using Molecular I/O for Sensing, Actuation, and Interaction. In *Proceedings of the CHI 2017*, 989-1000.
11. Karagozler, M.E., Poupyrev, I., Fedder, G.K., Suzuki, Y. 2013. Paper generators: harvesting energy from touching, rubbing and sliding. In *Proceedings of the UIST 2013*, 23-30.
12. Khalilbeigi, M., Lissermann, R., Kleine, W., Steimle, J. 2012. FoldMe: interacting with double-sided foldable displays. In *Proceedings of the TEI 2012*, 33-40.
13. Koizumi, N., Yasu, K., Liu, A., Sugimoto, M., Inami, M. 2010. Animated paper: A toolkit for building moving toys. *Computers in Entertainment (CIE) 8*, 7.
14. Liu, Y., Boyles, J.K., Genzer, J., Dickey, M.D. 2012. Self-folding of polymer sheets using local light absorption. *Soft Matter 8*, 1764-1769.
15. Liu, Y., Shaw, B., Dickey, M.D., Genzer, J. 2017. Sequential self-folding of polymer sheets. *Science Advances 3*, e1602417.
16. Lo, J., Paulos, E. 2014. ShrinkyCircuits: sketching, shrinking, and formgiving for electronic circuits. In *Proceedings of the UIST 2014*, 291-299.
17. Miyashita, S., Meeker, L., Tolley, M.T., Wood, R.J., Rus, D. 2014. Self-folding miniature elastic electric devices. *Smart Materials and Structures 23*, 094005.
18. Niiyama, R., Sun, X., Yao, L., Ishii, H., Rus, D., Kim, S. 2015. Sticky actuator: Free-form planar actuators for animated objects. In *Proceedings of the TEI 2015*, 77-84.
19. Ogata, M., Fukumoto, M. 2015. FluxPaper: reinventing paper with dynamic actuation powered by magnetic flux. In *Proceedings of the CHI 2015*, 29-38.
20. Olberding, S., Soto Ortega, S., Hildebrandt, K., Steimle, J. 2015. Foldio: Digital fabrication of interactive and shape-changing objects with foldable printed electronics. In *Proceedings of the UIST 2015*, 223-232.
21. Ou, J., Dublon, G., Cheng, C.-Y., Heibeck, F., Willis, K., Ishii, H. 2016. Cilllia: 3D printed micro-pillar structures for surface texture, actuation and sensing. In *Proceedings of the CHI 2016*, 5753-5764.
22. Ou, J., Skouras, M., Vlavianos, N., Heibeck, F., Cheng, C.-Y., Peters, J., Ishii, H. 2016. aeroMorph-Heat-sealing Inflatable Shape-change Materials for Interaction Design. In *Proceedings of the UIST 2016*, 121-132.
23. Paik, J.K., Kramer, R.K., Wood, R.J. 2011. Stretchable circuits and sensors for robotic origami. In *Proceedings of the 2011 IEEE/RSJ International Conference on Intelligent Robots and Systems (IROS)*, 414-420.
24. Probst, K., Seifried, T., Haller, M., Yasu, K., Sugimoto, M., Inami, M. 2011. Move-it: interactive sticky notes actuated by shape memory alloys. In *Proceedings of the CHI'11 Extended Abstracts on Human Factors in Computing Systems*, 1393-1398.
25. Qi, J., Buechley, L. 2012. Animating paper using shape memory alloys. In *Proceedings of the CHI 2012*, 749-752.
26. Qi, J., Buechley, L. 2010. Electronic popables: exploring paper-based computing through an interactive pop-up book. In *Proceedings of the TEI 2010*, 121-128.
27. Ratna, D., Karger-Kocsis, J. 2008. Recent advances in shape memory polymers and composites: a review. *Journal of Materials Science 43*, 254-269.
28. Sareen, H., Umapathi, U., Shin, P., Kakehi, Y., Ou, J., Ishii, H., Maes, P. 2017. Printflatables: Printing Human-Scale, Functional and Dynamic Inflatable Objects. In *Proceedings of the CHI 2017*, 3669-3680.

29. Saul, G., Xu, C., Gross, M.D. 2010. Interactive paper devices: end-user design & fabrication. In *Proceedings of the TEI 2010*, 205-212.
30. Shin, B., Felton, S.M., Tolley, M.T., Wood, R.J. 2014. Self-assembling sensors for printable machines. In *Proceedings of the 2014 IEEE International Conference on Robotics and Automation (ICRA)*, 4417-4422.
31. Tao, Y., Wang, G., Zhang, C., Lu, N., Zhang, X., Yao, C., Ying, F. 2017. WeaveMesh: A Low-Fidelity and Low-Cost Prototyping Approach for 3D Models Created by Flexible Assembly. In *Proceedings of the CHI 2017*, 509-518.
32. Tolley, M.T., Felton, S.M., Miyashita, S., Aukes, D., Rus, D., Wood, R.J. 2014. Self-folding origami: shape memory composites activated by uniform heating. *Smart Materials and Structures 23*, 094006.
33. Wang, G., Yao, L., Wang, W., Ou, J., Cheng, C.-Y., Ishii, H. 2016. xPrint: A Modularized Liquid Printer for Smart Materials Deposition. In *Proceedings of the CHI 2016*, 5743-5752.
34. Wang, W., Yao, L., Zhang, T., Cheng, C.-Y., Levine, D., Ishii, H. 2017. Transformative Appetite: Shape-Changing Food Transforms from 2D to 3D by Water Interaction through Cooking. In *Proceedings of the CHI 2017*, 6123-6132.
35. Wiethoff, A., Schneider, H., Rohs, M., Butz, A., Greenberg, S. 2012. Sketch-a-TUI: low cost prototyping of tangible interactions using cardboard and conductive ink. In *Proceedings of the TEI 2012*, 309-312.
36. Yakacki, C.M., Shandas, R., Lanning, C., Rech, B., Eckstein, A., Gall, K. 2007. Unconstrained recovery characterization of shape-memory polymer networks for cardiovascular applications. *Biomaterials 28*, 2255-2263.
37. Yakacki, C.M., Shandas, R., Safranski, D., Ortega, A.M., Sassaman, K., Gall, K. 2008. Strong, Tailored, Biocompatible Shape-Memory Polymer Networks. *Advanced functional materials 18*, 2428-2435.
38. Yao, L., Niiyama, R., Ou, J., Follmer, S., Della Silva, C., Ishii, H. 2013. PneUI: pneumatically actuated soft composite materials for shape changing interfaces. In *Proceedings of the UIST 2013*, 13-22.
39. Yao, L., Ou, J., Cheng, C.-Y., Steiner, H., Wang, W., Wang, G., Ishii, H. 2015. BioLogic: natto cells as nanoactuators for shape changing interfaces. In *Proceedings of the CHI 2015*, 1-10.
40. Yasu, K., Inami, M. 2012. Popapy: instant paper craft made up in a microwave oven. *Advances in Computer Entertainment*, 406-420.
41. Zhang, Q., Yan, D., Zhang, K., Hu, G. 2015. Pattern transformation of heat-shrinkable polymer by three-dimensional (3D) printing technique. *Scientific reports 5*.
42. Zhang, Q., Zhang, K., Hu, G. 2016. Smart three-dimensional lightweight structure triggered from a thin composite sheet via 3D printing technique. *Scientific reports 6*, 22431.